

SECONDARY ELECTRON YIELDS FROM THERMAL-SPRAYED METAL SURFACES AND MONTE CARLO SIMULATION OF SEY FROM ROUGH SURFACES

M. L. Yao[†], SOKENDAI, Tsukuba, Ibaraki, Japan

Y. Suetsugu¹, K. Shibata¹, H. Hisamatsu, T. Ishibashi¹, S. Terui, KEK, Tsukuba, Ibaraki, Japan

¹also at SOKENDAI, Tsukuba, Ibaraki, Japan

T. Nishidono, H. Chiba, Komiyama Electron Corp., Minamitsuru, Yamanashi, Japan

T. Sawahata, K. Ishii, MTC, Mito, Ibaraki, Japan

Abstract

We coated the copper substrates with copper by thermal spraying, and investigated the relations between their secondary electron yield (SEY or δ), roughness and surface composition. After enough conditioning, all the values of maximum SEY (δ_{\max}) were lower, and the energies of the primary electrons that gives δ_{\max} (E_{\max}) were higher than the flat surfaces. For the copper samples, it was found that the δ_{\max} and Sa divided by the developed interfacial area ratio (Sdr), Sa/Sdr, were in inverse proportion. Besides, we used Monte Carlo method to simulate the SEY of rough copper surface. In the simulation, the relationship between δ_{\max} and Sa/Sdr was inconsistent with the experimental results. Furthermore, we applied the thermal spray to grooves and measured the SEYs from them. A lower δ_{\max} was obtained even in a blunt groove. Even more interesting in this case, the measured and simulated δ_{\max} were qualitatively in agreement.

INTRODUCTION

It has been well known that the electron cloud effect (ECE) in a positron or proton ring seriously deteriorate the performance of the collider, i.e., luminosity [1, 2]. The secondary electron yield (SEY or δ) is a primary parameter for controlling the ECE. One of the applicable solutions would be preparing a material with a low SEY on the inner surface of beam pipes.

A rough surface generally has a lower SEY than a smooth surface, and the roughening methods include machining, chemical reaction, laser abrasion, etc. The emitted secondary electrons are likely to be captured on the rough surface, and then the effective SEY should be reduced.

In this study, we investigated the SEY properties from the thermal-sprayed copper surfaces [3]. Thermal spraying is an easy method to practice and has been widely used in industries, here this technology is used for the first time to reduce the SEY. The relations between the SEY properties and the roughness parameters were investigated. Furthermore, we tried to explain the results by the numerical simulations using several SEY models. Finally, we applied the thermal spray method to grooved surface, and measured SEY from them. The experimental and simulation results were compared again.

EXPERIMENTAL

Sample Preparation

In this study, copper substrates were coated with copper powder by plasma formed by argon and hydrogen. The substrate is a disk with a diameter of approximately 15 mm and a thickness of 3 mm. Copper is a relatively stable material compared to aluminum, and it is easier to process than stainless steel. Therefore, we mainly used copper as the research object.

Twelve different thermal-sprayed samples listed in Table 1 were prepared [3]. Two different sizes of copper powder were used for thermal spraying. The diameter of the bigger one is 125 - 170 μm (the samples are referred by "B" in the table) and the smaller one is 45 - 50 μm (the samples are referred by "S" in the table).

As for the substrate pre-treatment, except for the normal machined surface ($R_a = 1.14 \mu\text{m}$), glass beads blast (GBB, $R_a = 8.14 \mu\text{m}$) was used to enhance the coating adhesion. The samples that had been treated with GBB were marked as "GBB". In sample B_LT, B_GBB_LT, S_LT and S_GBB_LT, we simply used argon without mixing hydrogen as the plasma source to lower the plasma temperature, and these samples were marked as "LT".

Furthermore, in order to increase the roughness of the surface, we made two special patterns of the coating. The first one is a trench. The samples B_GBBpre_trench and S_GBBpre_trench were coated with a "trench" in the middle of the sample surface, of which depth is 50 μm and the width is 2 mm. First, we applied a coating on the surfaces evenly (which was called "pre-spray" after GBB in this report and marked as "GBBpre"), then used a metal sheet as a baffle to perform the thermal spraying, leaving a trench in the middle of the samples.

The second pattern is a mesh. In samples B_GBB_mesh, B_GBBpre_mesh, S_GBB_mesh and S_GBBpre_mesh, we used a metal mesh as a baffle to do the thermal spraying. The aperture and wire diameter of the mesh are 0.597 and 0.25 mm respectively. Samples B_GBBpre_mesh and S_GBBpre_mesh had a uniform coating before the meshed spraying, and B_GBB_mesh and S_GBB_mesh were directly performed the mesh spraying after the GBB.

[†] yaomulee@post.kek.jp

Table 1: Copper Samples

	Sub- strate	Substrate pre-treatment	Powder size (μm)	Plasma- forming gas	Special pattern	Sa (μm)	Sdr
B_STD	Cu	Machined		Ar + H ₂		25.96	0.28
B_LT	Cu	Machined	Big	Ar		3.77	0.07
B_GBB_LT	Cu	GBB	(diameter	Ar		12.32	0.22
B_GBBpre_trench	Cu	GBB+pre-spray	125-170)	Ar + H ₂	Trench	14.94	0.23
B_GBB_mesh	Cu	GBB		Ar + H ₂	Mesh	28.57	0.19
B_GBBpre_mesh	Cu	GBB+pre-spray		Ar + H ₂	Mesh	22.42	0.17
S_STD	Cu	Machined		Ar + H ₂		5.44	0.11
S_LT	Cu	Machined	Small	Ar		8.43	0.17
S_GBB_LT	Cu	GBB	(diameter	Ar		10.55	0.20
S_GBBpre_trench	Cu	GBB+pre-spray	45-50)	Ar + H ₂	Trench	6.12	0.11
S_GBB_mesh	Cu	GBB		Ar + H ₂	Mesh	25.40	0.12
S_GBBpre_mesh	Cu	GBB+pre-spray		Ar + H ₂	Mesh	26.20	0.11
Cu flat						3.28	0.23

Experiment

Here we list all the items of the experiments we have done. For detailed settings, please refer to our previous report [3].

Roughness parameters measurement The measured parameters include Sa (arithmetical mean height), Sq (root mean square height), Sz (maximum height), Sdr (developed interfacial area ratio), etc [4].

SEM image measurement The typical magnifications we used were 100 [3].

Surface composition analysis The surface compositions of the copper samples B_GBB_LT, B_GBBpre_trench, S_GBB_LT and S_GBBpre_trench were investigated after the SEY measurement by using XPS at Komiyama Electron Corp. The results showed that there was no significant difference in the surface composition in these four copper samples. The main component of the surface was cuprous oxide (Cu₂O), and some amorphous carbon and graphite produced by conditioning were detected. From this, it could be inferred that the difference in SEY of these copper samples after the conditioning are mainly caused by the surface topography.

SEY measurement The measurement started after a baking at 160 °C for 24 hours and the typical working pressure is at the level of 10⁻⁷ Pa. The SEY of each sample was measured within 150 - 2000 eV of primary electron energy (E_p) after the conditioning time of 2, 7, 24 and 48 hours. The E_p during the conditioning was 350 eV. After 48 hours conditioning, the total electron dose reached to $\approx 6 \times 10^{-2}$ C/mm² [3].

MONTE CARLO SIMULATION OF SEY FROM ROUGH SURFACES

Composition of Secondary Electrons

The conventional picture of secondary emission can be summarized as follows [5]: when a steady electron current I_0 impinges on a surface, a certain portion I_e is backscattered elastically while the rest penetrates into the material. Some of these electrons are scattered by one or more atoms

inside the material and are reflected back out. These are the so-called “re-diffused” electrons, and we call the corresponding current I_r . The rest of the electrons interact in a more complicated way with the material and yield the so-called “true-secondary electrons,” the current of which we refer as I_{ts} . The yields for each type of electron are defined by $\delta_e = I_e/I_0$, $\delta_r = I_r/I_0$, and $\delta_{ts} = I_{ts}/I_0$, so that the total SEY (δ) is:

$$\delta = \frac{I_e + I_r + I_{ts}}{I_0} = \delta_e + \delta_r + \delta_{ts} \quad (1)$$

Usually, the δ_r is much smaller than δ_{ts} ($E_p \sim 40$ eV) or δ_e ($E_p < \sim 40$ eV), so here we neglected this portion in the simulation. We consider the δ for two cases depending on the incident electron energy E_p as follows:

$$\delta(E_p, \theta) \approx \delta_{ts}(E_p, \theta) \text{ for } E_p > \sim 40 \text{ eV} \quad (2)$$

$$\delta(E_p, \theta) \approx \delta_e(E_p) \text{ for } E_p < \sim 40 \text{ eV} \quad (3)$$

The δ_e can be modeled as follows:

$$\delta_e(E_p) = R_0 \frac{(\sqrt{E_p} - \sqrt{E_p + E_0})^2}{(\sqrt{E_p} + \sqrt{E_p + E_0})^2} \quad (4)$$

with two fit parameters E_0 and R_0 . The R_0 is the reflectivity at zero impinging energy, which is typically 0.8. The value of E_0 should be determined from the measured data, but typically 150 eV. We neglected the angle dependence of δ_e because it is weak.

For the δ_{ts} , after referring to several SEY models, the SEY model derived by Furman [5] was chosen to describe the δ_{ts} in our simulation, which is based on a broad phenomenological fit to data for the secondary-emission yield. The δ_{ts} value is given by:

$$\delta_{ts} = \delta_{max} \frac{s \frac{E_p}{E_{max}}}{s - 1 + \left(\frac{E_p}{E_{max}}\right)^s} \quad (5)$$

here s is an adjustable parameter that must be > 1 . For off-normal incidence of the primary electrons, the δ dependence of the δ_{\max} and E_{\max} are:

$$E_{\max}(\theta) = E_{\max}(0)(1 + 0.7(1 - \cos\theta)) \quad (6)$$

$$\delta_{\max}(\theta) = \delta_{\max}(0)\exp(\gamma(1 - \cos\theta)) \quad (7)$$

Here γ is a constant and is typically 1/2.

SEY Simulation from Rough Surfaces Using VBA

We developed a three-dimensional Monte Carlo simulation code to calculate “effective δ ” from the rough surface using the formulae described in the previous section. The code was written in Excel Visual Basic for Application (Excel VBA). Total number of escaped secondary electrons is the “effective δ ” from the surface in question.

In the simulation, a primary electron is injected vertically onto the surface ($y = 0$ plane) at first. The emission of secondary electrons is calculated following the formula described in the previous subsection. A secondary electron is traced until it is adsorbed on the surface or it run away from the surface ($y > 0.1$ mm). The ratio of the number of run-away electrons and that of incident electrons are calculated as the δ . Main parameters and assumptions used in the calculation are as follows:

1. Sample size is 8 mm \times 8 mm (square).
2. Beam size of the primary electron is 4 mm \times 4 mm (square) at the center of the sample. The incident point is randomly chosen over the ranges of the beam size.
3. E_p ranges from 50 to 2,000 eV with a step of 50 eV.
4. Typical number of primary electrons for each E_p is 8,000 and the electrons are randomly incident in the range of the beam size.
5. Range of incident angle θ is $0 \leq \theta < 90^\circ$, where $\theta = 0^\circ$ means the normal incidence.
6. Range of the energy of the secondary electrons is 5 ~ 15 eV. The energy distribution is uniform within this range.
7. The emission direction of the secondary electrons obeys the cosine distribution.
8. Calculated roughness parameters are Sa, Sq, Sz, Sdr.

Trapezoidal protrusions

The SEM observation of the sample surface indicated that the thermal-sprayed surfaces do not have sharp protrusions [3]. The shape of the peak and valley of the protrusions were not sharp, and the sides were not normal to the surface. From these considerations, trapezoidal protrusion surfaces were constructed to roughly imitate the real thermal-sprayed surfaces.

Figure 1 shows the pattern of how we change the parameters of the trapezoidal protrusion models. The Sz varies from 50 to 300 μm with a step of 50 μm , and the θ varies in 30° , 45° , 60° and 80° . The width of the peak and valley is Sz divided by $\tan\psi$, where $\psi = 30^\circ$, 45° , 60° and 80° . Therefore 96 different trapezoidal protrusions were constructed. Figure 2 shows an example of the model of the trapezoidal protrusions.

- ①Sz: 50, 100, 150, 200, 250, 300 μm
- ② θ : 30° , 45° , 60° , 80°
- ③width = Sz / $\tan\psi$, ψ : 30° , 45° , 60° , 80°

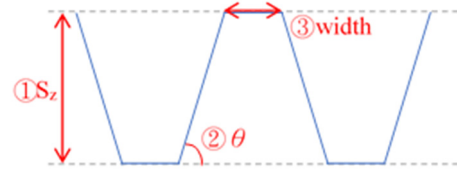


Figure 1: Parameters of the trapezoidal protrusions.

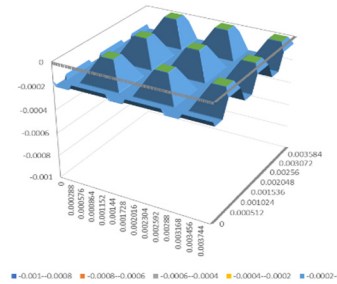


Figure 2: Model of the trapezoidal protrusions.

RESULTS AND DISCUSSIONS

SEY Measurement

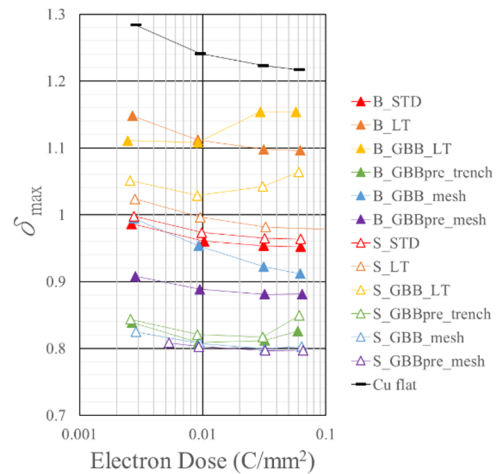


Figure 3: The δ_{\max} of Cu samples as a function of electron dose.

Figure 3 shows the δ_{\max} of the copper samples as a function of electron dose after 48 hours conditioning as a function of the electron dose. As a whole, all the δ_{\max} of the thermal-sprayed copper surfaces were lower than that of the flat copper surface, as expected. The energies of the primary electrons that gives δ_{\max} (E_{\max}) were higher than the flat surfaces. Generally, the δ_{\max} was lower for the “S”-type samples than for the “B”-type samples. For the case of samples (B_STD, S_STD) and (B_GBBpre_trench, S_GBBpre_trench), the δ_{\max} were almost the same. The meshed samples (S_GBB_mesh, S_GBBpre_mesh) had the lowest value of δ_{\max} .

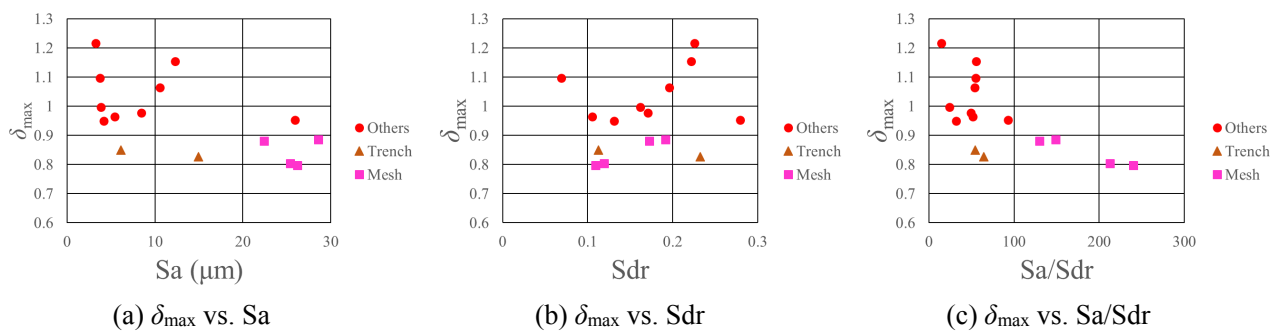


Figure 4: The final δ_{\max} of Cu samples as a function of roughness parameters.

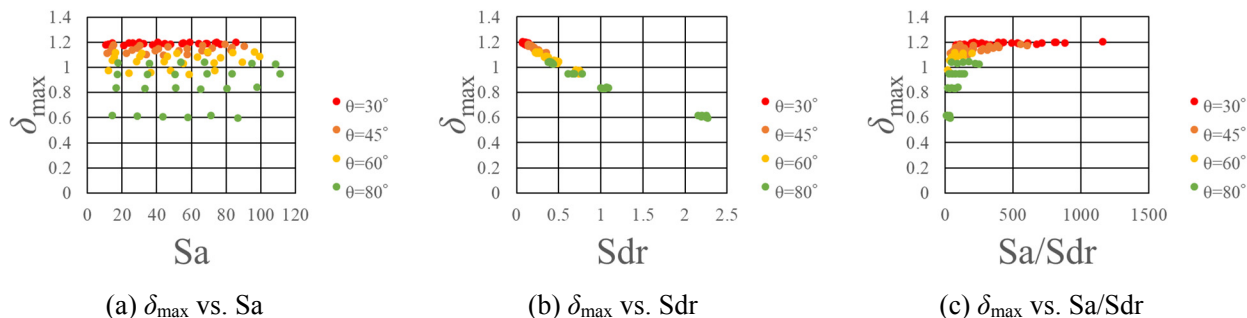


Figure 5: The profiles of simulated δ against the roughness parameters of the copper trapezoidal protrusions.

For the “LT” samples, the coatings of samples (S_LT, S_GBB_LT), where the smaller powders were used, kept the bead shape successfully, but the coatings of samples (B_LT, B_GBB_LT), where the bigger powders were used, lost the bead shape and melt on the surface. However, the δ_{\max} of (S_LT, S_GBB_LT) were only slightly lower than that of (B_LT, B_GBB_LT), and all of them were higher than that of (B_STD, S_STD). This may be related to the incompleteness of the distribution of the particles that retain the spherical shape.

Another interesting phenomenon was observed in the samples (B_GBB_LT, S_GBB_LT) and (B_GBBpre_trench, S_GBBpre_trench). The δ_{\max} of these four samples increased with the conditioning time. Now we suspect that these rising SEYs are due to the reduction of Cu_2O to Cu on the thermal-sprayed surfaces. But this cannot explain why only the SEY of these four samples rose with the exposure of electron beam. Further investigation is required.

Roughness parameters and SEY

Many roughness parameters had been compared to the δ_{\max} , but only some parameters appeared to be relevant. Figure 4 shows the relationship between the final δ_{\max} and the roughness parameter of Sa, Sdr and Sa/Sdr for copper samples. No obvious dependence of δ_{\max} on the Sa or Sdr was found, but the δ_{\max} had evident negative correlation to Sa/Sdr.

On the other hand, in the results of simulation for the copper trapezoidal protrusions as shown in Fig. 5, the δ_{\max} changed with the sharpness of the protrusions, i.e. larger θ and shorter width, and was independent of the scale of the structure. It was obvious that the δ_{\max} had strong negative

correlation to “Sdr”, but not “Sa/Sdr”, which is different from the experiment.

We consider the following two possible reasons for this difference; (1) Instrument limitations: The different dependence on Sdr should be due to the resolution limit of our 3D measuring microscope. For Sa, it needs the height of particles, which is easier to obtain even for low resolution. But Sdr needs the lengths of slopes of the melted metal particles on the surface, which is difficult to measure with our resolution. We found that under different magnifications, Sa was almost the same, and the variation of Sdr was quite large, which proved that our instrument has insufficient resolution for Sdr. (2) Diversity of the surface pattern: We found that the patterns with different surface shapes have different slope of δ_{\max} against Sdr, for example, the slope of the trend of the triangular protrusion and the trapezoidal protrusion was not the same. And due to the different thermal-sprayed conditions, the pattern of the surface shape may vary greatly. From this standpoint, the trend in Fig. 4(c) should be just a coincidence.

APPLICATION TO GROOVED SURFACES

We applied the thermal-sprayed coating to groove surfaces. Prepared samples are:

1. Sharp groove
2. Blunt groove
3. Blunt groove + Thermal spray
4. Blunt groove + Thermal spray + TiN coating

The schematic cross sections of structures 1 and 2 are shown in Fig. 6. It is reported that a groove with a sharper peak/valley and a narrower angle generally has a lower δ_{\max} . However, from a practical point of view, the manufacturing

of a sharp groove is more difficult than that of a blunt groove.

Figure 7 shows the δ_{\max} of the four samples after 48 hours conditioning as a function of the electron dose. As shown in the figure, the δ_{\max} of the blunt groove with the thermal-sprayed coating is almost the same to the sharp groove. It is a big merit of the thermal spray. By applying TiN coating further on the thermal-sprayed surface, the δ_{\max} lowered further even in the blunt groove.

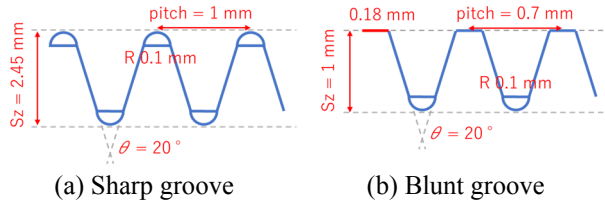


Figure 6: Cross sections of (a) sharp groove and (b) blunt groove.

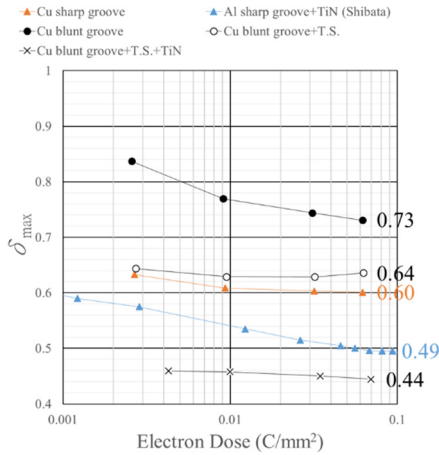


Figure 7: The final δ_{\max} of the four groove samples as a function of electron dose.

The SEYs for these four grooved structures were simulated using the surfaces with following parameters, where the arcs at the bottoms and tops of the grooves were replaced by polygons, i.e., trapezoids, for simplicity;

1. $\delta_{\max} = 1.217$, $E_{\max} = 450$ eV and $s = 1.5$
2. $\delta_{\max} = 1.217$, $E_{\max} = 450$ eV and $s = 1.5$
3. $\delta_{\max} = 0.9636$, $E_{\max} = 650$ eV and $s = 1.45$, which were obtained by fitting the experimental result of S_STD.
4. $\delta_{\max} = 0.6016$, $E_{\max} = 700$ eV and $s = 1.2$, which were obtained by fitting the experimental result.

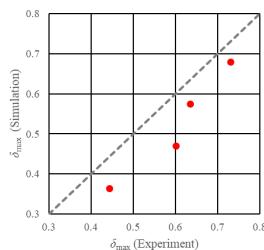


Figure 8: Correlation between the simulated and measured δ_{\max} for the four grooved samples.

Figure 8 presents the correlations between measured δ_{\max} and the simulated ones for these four samples. As shown in this figure, a good correlation was obtained, although the δ_{\max} of the simulation were always lower than those of measurements. This indicated that the present simulation can qualitatively evaluate the SEY from the global rough surfaces, such as groove structure.

CONCLUSION

For the SEY measurement, all the δ_{\max} of the thermal-sprayed copper surfaces were lower than that of the flat surface, and generally the δ_{\max} was lower for the “S”-type samples than for the “B”-type samples. The E_{\max} became higher and the δ profiles were broader for the thermal-sprayed surfaces compared to the case of flat surface. In the copper samples, the meshed samples had the lowest δ_{\max} and can reduce the δ_{\max} from ≈ 1.2 to ≈ 0.8 . For the roughness measurement of copper samples, the δ_{\max} had evident negative correlation to Sa/Sdr.

In the simulation, it was found that if the boundary of the surface protrusion is more well-defined and sharper, a lower SEY is obtained. In the results of simulation, the δ_{\max} had strong negative correlation to “Sdr”, but not “Sa/Sdr”, which was not consistent to the experimental results. We infer that is caused by the insufficient resolution of the 3D measuring microscope and the diversity of the surface pattern of the thermal-sprayed surfaces, since the patterns with different surface patterns should have different slopes of δ_{\max} against Sdr.

The thermal-sprayed groove shows a low SEY even a blunt groove. This can be a big merit in manufacturing grooves in a practical long beam pipes, where making a sharp groove is hardly possible. Furthermore, a good correlation was obtained between the measured and simulated δ_{\max} . These results indicate that the present simulation is able to make a qualitative prediction of SEY for the simple periodic rough surface. Further investigation will be required to understand these discrepancies between the simulation and the experiments.

REFERENCES

- [1] Zimmermann, H. Fukuma, and K. Ohmi, “More electron cloud studies for KEKB: Long-term evolution, solenoid patterns, and fast blowup”, CERN Report No. CERN-SL-Note-2000-061 AP, Dec. 2000.
- [2] H. Fukuma *et al.*, “Observation of vertical beam blow-up in KEKB low energy ring”, in *Proc. EPAC2000*, Vienna, Austria, Jun. 2000, pp. 1122-1124.
- [3] M. Yao *et al.*, “Secondary electron yields from thermal sprayed metal surfaces”, in *Proc. PASJ2018*, Nagaoka, Japan, Aug. 7-10, 2018, paper WEP113, pp. 649-653.
- [4] Keyence, <https://www.keyence.com/ss/products/microscope/roughness/surface/parameters.jsp>
- [5] M. A. Furman and M. T. F. Pivi, “Probabilistic model for the simulation of secondary electron emission,” *Phys. Rev. ST Accel. Beams*, vol. 5, p.124404, Dec. 2002.